A study on the effect of print parameters on mechanical properties of parts manufactured using additive manufacturing

by

Elisa Aznarte Garcia

A thesis submitted in partial fulfillment of the requirements for the degree of

Master of Science

Department of Mechanical Engineering
University of Alberta

Abstract

This thesis presents an investigation on material-process interaction of vat-photopolymerization processes. The effect of different printing factors on tensile properties is studied. Two vat-photopolymerization processes are considered: Digital Light Processing (DLP) and Stereolithography (SLA). A comprehensive list of factors available on the slicing software and other factors, like the orientation of the part or its position, are investigated. To perform this study, Design of Experiments (DoE) is introduced by the use of Taguchi's techniques. The relationship between each factor and the elastic modulus, ultimate tensile stress, and strain at break is obtained. Furthermore, the total print time is analyzed with respect to the obtained mechanical properties. The study indicates that part orientation, exposure time to the UV light and layer thickness are the most important factors affecting the investigated properties. The last section of this thesis highlights the main differences found between the studied processes.

Preface

(Mandatory due to journal)

A version of Chapter 2 of this thesis will be submitted for as a journal publication in 3D Printing and Additive Manufacturing Journal. The authors of the publication are E. Aznarte, A.J. Qureshi, and C. Ayranci, and the title is "Material-Process Interaction Optimization Of Vat-Photopolymerization Process". The work included in this chapter represents the design, testing and results interpretation done by me under the guidance of Drs. Ayranci and Qureshi.

A version of Chapter 3 of this thesis is being prepared to be submitted as a journal publication to Rapid Prototyping Journal. Authors of the paper will be E. Aznarte, and C. Ayranci, A.J. Qureshi, and the title of the paper is planned to be "Tensile Consideration on Stereolithography Vat-Photopolymerization". The work included in this chapter represents the design, testing and results interpretation done by me under the guidance of my supervisors, C. Ayranci and A.J. Qureshi.

Acknowledgments

I would like to thank my Master Supervisors Dr. Cagri Ayranci, and Dr. Ahmed Qureshi, for their guidance and support during my studies.

I would also like to acknowledge the institutions that made my research possible; University of Alberta, Natural Sciences and Engineering Research Council of Canada (NSERC) and Canadian Foundation for Innovation (CFI).

Lastly, I must say thank you to my family, for all the opportunities and love that I received over the years.

Table of Contents

List of Tables

List of Figures

CHAPTER 1 INTRODUCTION

1.1. MOTIVATION

Additive Manufacturing (AM) is a process used to produce three-dimensional (3D) parts using a layer-by-layer material deposition techniques [1]. AM, also known as 3D printing, was initially developed as a prototyping tool that allowed design concepts' verification using a piece that is drawn in a Computer Aided Design (CAD) file. 3D printing, enables the fast creation of virtually any complex shape at a low cost compared to other traditional manufacturing methods, such as injection molding, casting, and the like.

Several machines that allow different types of AM processes are available for non-industrial users in a desktop version; for example, Extrusion Based Additive Manufacturing (EBAM) (also known as Fused Deposition Modeling (FDM) or Fused Filament Fabrication (FFF)), Selective Laser Sintering (SLS), Stereolithography (SLA) and Digital Light Processing (DLP) machines. This research is focused on the effect of print parameters on mechanical properties of Stereolithography (SLA) and Digital Light Processing (DLP) based machines that fall under Vat photopolymerization.

Vat photopolymerization techniques use a tank, or bath, of polymeric photosensitive resin. Stereolithography was invented and patented by Charles Hull in 1982 and 1986 respectively [2]. SLA uses an Ultraviolet (UV) light to cure photosensitive resin within a given pattern that is extracted from the STL file and corresponds to one layer of the printed part [3].

There are infinite combinations of ingredients that can create infinite types of resins, the main components are a monomer material, a photoinitiator and an absorber [4]. The process of linking monomers into polymers initiated by radiation exposure is known as photopolymerization; and, it can be divided into three steps: initiation, propagation and termination [5]. The source of the radiation in charge of the photopolymerization is typically a laser beam or a Digital Light Processor (DLP); that, given the exothermicity of the photopolymerization does not need to be a high-power light source [5]. In general, two of the most common parameters to be controlled during cross-linking process are the layer thickness and the exposure time of light [6].

Parts manufactured by vat photopolymerization do not have consistent mechanical properties. These properties depend mostly on the curing process of the resin, which is affected by the

power of the light source, the wavelength, the speed of construction, the resin composition and other factors [7]. For example, a specimen subjected to a low exposure time will probably not be fully cured; hence, it would break at low stresses in tension.

1.2. THESIS OBJECTIVE

The primary objective of this research is to understand and optimize the printing parameters' effect on mechanical properties of printed parts using DLP and SLA techniques. The quantification of the effect is achieved through design of experiments (DoE). This work includes tensile test specimens design and manufacturing according to the designed experiments. Similar studies are available for Electron Beam Additive Manufacturing (EBAM) type printing machines; however, this data is much limited for vat-photopolymerization machines. Consequently, the findings of this study will fill a knowledge gap in literature, and inform and guide engineers and scientists working in the field for research and design purposes.

1.3. THESIS OUTLINE

This thesis is organized into four chapters. Chapters 2 and 3 are written in journal format; where first background information regarding main aspects of additive manufacturing (AM) and vat-photopolymerization processes are presented. Then, the methodology and materials used are outlined. Later, the experimental processes are described and a detailed analysis of results is performed. Finally, all results are discussed in the order of appearance in the papers followed by a conclusions section that extracts the most important findings of each study.

In Chapter 4, a tabulated summary of results is presented with a general conclusions section. Recommendations for future studies are given, as well as the limitations of this thesis and suggestions for future work.

CHAPTER 2 MATERIAL-PROCESS INTERACTION OPTIMIZATION OF VAT-PHOTOPOLYMERIZATION PROCESS (*)

(*) A version of this chapter will be submitted to 3D Printing and Additive Manufacturing Journal as a journal paper with the authors: Elisa Aznarte Garcia, A.J. Qureshi, Cagri Ayranci

2.1. INTRODUCTION

Additive Manufacturing (AM) is a group of advanced manufacturing technologies for producing parts from a three-dimensional (3D) Computer Aided Design (CAD) model using a layer-by-layer material deposition approach. Due to this fabrication approach, the resulting parts exhibit anisotropy in mechanical properties. The consideration of this anisotropy in integrated design and manufacturing via AM is one of the main barriers to overcome to main-stream uptake of this technology.

There are a number of previous studies on mechanical properties and geometric variations in relation to the printing parameters based on various AM technologies such as Fused Deposition Modeling (FDM) or Fused Filament Fabrication (FFF) [8]–[11]; however, there is limited literature on mechanical properties of parts obtained through vat photopolymerization.

Examples of previous research showed that, for FFF printed at different orientations the UTS is higher for parts with fibers aligned with the tensile force direction rather than perpendicular to this direction [8]. Others, performed similar studies including variations in the layer thickness with the objective of comparing commercial and open source FDM printers [11]. Finally, some researchers also considered the printed part scale, that resulted to be a high relevant factor when analyzing 3D printed parts [9].

The objective of this study is to investigate the effect of the process parameters on the properties of parts produced via Vat Photopolymerization processes and find the optimal parameter values. The properties considered were elastic modulus, ultimate tensile strength (UTS), and ultimate strain. In addition to mechanical properties, printing time was also considered. The principal reason for including the printing time in this research is its direct contribution to cost of printing the part and subsequently the cost of achieving a specific engineered mechanical property.

Taguchi's design is a common tool used in experimental analysis to optimize a process that is sensitive to changes of the process parameters. Taguchi's techniques are based on statistical design of experiments and address the need of reducing cost or maximizing the output under certain restrictions. Based on the Taguchi's design of experiments along with the aforementioned mechanical properties a systematic process model is presented to optimize the mechanical properties and the printing time. To complete the results, one extra set of experiments is performed on specimens subjected to a bath of UV light after printing. The findings will be extremely useful for use of design engineers in the field.

2.2. MATERIALS AND METHODOLOGY

2.2.1. Equipment

Printer: An Ember DLP® 3D printer by Autodesk was used for this study. Ember uses a Digital Micromirror Device (DMD) to project a 2-dimensional light-pattern for simultaneous layer curing. The DMD consists of an array of 912x1140 micromirrors in a diamond orientation. The light projected by the DMD has a wavelength of 405 nm with a total optical power of 5W. The resolution offered by the printer as per the technical specifications is 50µm along the printing plane, also called XY resolution, and 10µm along the plane perpendicular to the building surface, also known as Z resolution. The maximum building dimensions are 60x40x134mm (X, Y, Z). The printer's firmware version during the duration of the study was 3.0. The resin used in this study was PR-48, manufactured specially to be used with Ember Printer. Its commercial name is Autodesk Standard Clear Resin.

CAD software: All CAD models were created using SOLIDWORKS® 2015 by Dassault Systèmes.

Slicing software: Autodesk Print Studio v1.6.5 software was used to process the CAD models.

Data analysis software: MATLAB R2016a and Minitab® 17.3.1 were used to analyze the experimental data.

Universal Testing Machine: A Bose ElectroForce 3200 Test Instrument was used to perform the tensile tests. The machine was equipped with a 450 N capacity load cell.

2.2.2. Methodology

The 3D printer has a total of 64 controllable parameters that can be modified through the slicing software. The parameters are grouped within five main categories: support, general, first layer, burn-in layer, and model layer.

Support category is related to any additional structure that shall be added for adhesion forces and support purposes. These are necessary to maintain the part attached to the building surface. In some cases, a section of the printed part may float if the supports are not added or correctly attached. **General** category accounts for only three settings: anti-alias image boundary, strength exposure and homing approach. These settings are binary; i.e. they can either be activated or deactivated. They are further explained in the *Design of Experiment* subsection. **First Layer** category refers to all of the available printing parameters for the first layer that links the build plate and the printed part. There are 16 settings in this category that are repeated for the next two categories (Burn-in Layers and Model Layer) and most of them determine the maximum distance, velocity and acceleration of the physical movements of the machine. **Burn-in Layers** are the layers printed right after the first layer. This category includes the same 16 settings as the **First Layer** category and one extra parameter. This extra parameter designates the total number of burn-in layers, which is usually less than 10. Burn-in Layers undergo longer exposure times and are printed at lower speeds compared to the following layers in a print. Their purpose is to increase the adhesion between the first layer, and the rest of the layers, and the building surface. The **Model Layer** category includes the same 16 settings as the First Layer and controls the properties of the rest of the layers.

Addition to these categories, *part orientation* and *part rotation*, that refer to the alignment and orientation of the part in a 3-dimensional Cartesian coordinate with respect to the building surface, was also studied in this work.

2.2.2.1. Test Specimens

The tensile test specimens used for this work were printed in accordance with the ISO-527-1/2:2012 standard [12]. The maximum build size of the printer was the determining factor in the test specimen type, which was chosen as ISO527:Type 1BB. A schematic view and the dimensions of the specimen is shown in Figure 2.1

2.2.2.2. Design of Experiments

A set of 12 factors were considered for this study, three of them were two-level factors and 9 of them were three-level factors. The two-level factors were binary factors, while most of the three-level factors were defined as ±25% of the manufacturer recommended settings. Table 2.1 shows the factors considered. All the factors that refer to layer settings apply only to model-layers; all other factors were left as default.

Table 2.1 Factors implemented in Taguchi design of experiments

Factor number	Factor Name	Unit	Number of Levels	Level 1	Level 2	Level 3
1	Anti-Alias	-	2	Yes	No	-
2	Variable strength exposure	-	2	Yes	No	-
3	Part rotation (Spin)	-	2	X	Y	-
4	Layer thickness	µm	3	10	25	50
5	Wait (before exposure)	s	3	1.125	1.5	1.875
6	Exposure time	s	3	1.6	1.8	2
7	Separation slide velocity	rpm	3	6	8	10
8	Z-axis overlift	mm	3	0.5625	0.75	0.9375
9	Separation Z-axis velocity	mm/s	3	1.125	1.5	1.875
10	Approach slide velocity	rpm	3	9	12	15
11	Approach Z-axis velocity	mm/s	3	1.125	1.5	1.875
12	Part orientation	-	3	X	Y	Z

A brief explanation about each factor is given below:

Factor 1, **anti-alias**, refers to the smoothing of the edge of a part, achieving smoother surfaces by applying grey scale instead of full steps. *Factor 2*, **variable strength exposure**, applies when printing small and big features at the same time. Small features need more power to form while a greater section of resin needs less light power to complete, if this factor is activated small features will be represented on white while large features will be on a light grey color. *Factor 3*, **part orientation or spin**, refers to the rotation of the part with respect to its longitudinal axis; it

can be observed in Figure 2.1. *Factor 4*, **layer thickness,** refers to the height variation of the building platform between consecutive layers. *Factor 5*, **wait before exposure,** is the time that the resin tray and the building platform stay static just before exposing a new layer.

Factor 6, **exposure time**, is the total time that the light is being projected to cure a new layer of resin. *Factor 7*, **separation slide velocity**, is the velocity at which the resin tray rotates right after exposing the new layer. This rotation allows separating the new layer from the window of the tray. *Factor 8*, **Z-axis overlift,** is the distance that the building platform is raised between layers right after the separation rotation. *Factor 9*, **separation Z-axis velocity**, is the speed at which the Z-axis overlift happens. *Factor 10*, **approach slide velocity**, is the opposite rotation of factor 7. This rotation brings the tray back to the building position. *Factor 11*, **approach Z-axis velocity**, is the speed at which the building platform descends to achieve a distance equal to the layer thickness between its surface and the window of the tray. *Factor 12*, **part orientation**, refers to the alignment of the part with respect to the axis of the printer as shown in Figure 2.1.

The experimental matrix, based on Taguchi's mixed level design of experiments (DoE), was implemented in Minitab. Taguchi aims to minimize the noise factors' effect through the signal-to-noise ratio (S/N). Taguchi, through orthogonal arrays, gives combinations of factors and levels to generate a list of the minimum number of experiments [9]. On the other hand, some assumptions such as non-factor interactions must be made before the experiment is designed. Based on the factors considered, 36 different factorial experiments were conducted (Taguchi's array L36). Each experiment was simultaneously printed in a batch of five samples. This resulted in a total of 5x36=180 samples. The sample size was limited to 5 due to the print area constraint of the printer. All samples within an experiment were printed simultaneously for each run to establish the repeatability of the process. A secondary benefit of simultaneous sample printing was to establish in-plane dimensional and mechanical repeatability of the prints.

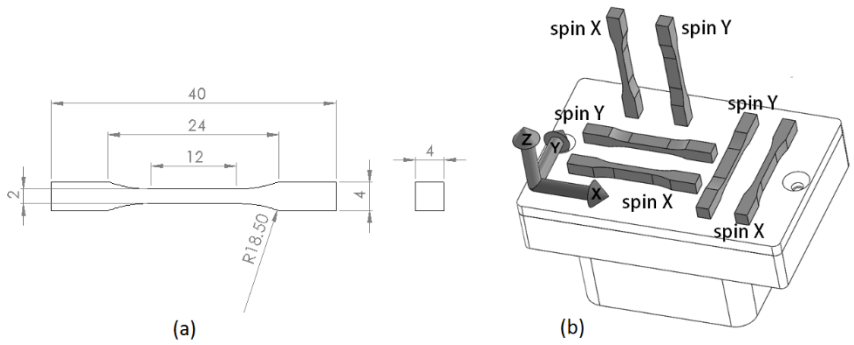

Figure 2.1 (a) ISO 527 specimen type 1BB and measurements (mm), (b) Building surface, part orientation and part rotation levels

2.2.2.3. Pre processing

The CAD files were saved in STL format, with a deviation tolerance of 0.002 mm and an angle tolerance of 0.5°, and were then imported in Print Studio to the building surface. Consequently, the models were sliced as per the DoE and saved as a compressed file. The files were then sent to the printer.

2.2.2.4. Post processing

The printed pieces were immersed in a 96% ethyl alcohol bath for 3 minutes following the manufacturer's recommendations to dissolve any excess liquid resin that may have remained on the part. The parts were subsequently left to air-dry for 24 hours.

2.2.2.5. Tensile testing

All the tensile tests were performed 24 hours after printing the specimens. The tests and the subsequent data analysis were done as per the ISO 527:2012 standard [12].

2.3. RESULTS AND DISCUSSION

During the printing process, two of the experiments were excluded due to the impossibility of finishing the printing process due to excessive jamming or other failures, the data placement corresponding to these experiments was left empty. This meant 34 batches instead of the planned 36. After the completion of the test, a total of 170 valid results were obtained.

The remaining data was analyzed and ranked in terms of S/N ratio and means response. Some information and histograms were also extracted from the population results.

2.3.1. General interpretation of the results

Figure 2.2 shows the elastic modulus boxplot for 34 batches tested. The average sample elastic moduli of the 34 sets of experiments varied between 0.39 GPa and 1.21 GPa. These numbers show increments of more than 214% for the same material printed using different parameters.

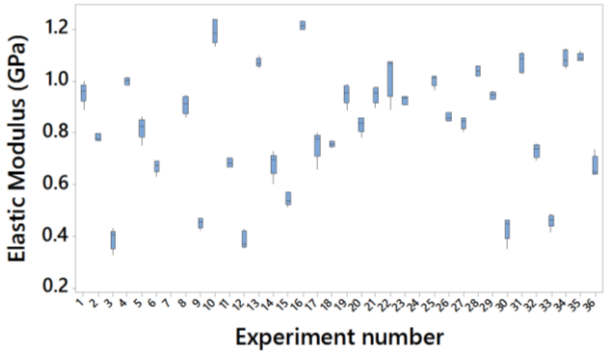

Figure 2.2 Boxplot of elastic moduli grouped in batches

Similarly, Figure 2.3 shows the distribution of average sample UTS of the 34 sets of experiments. The UTS mean values vary between 7.9 and 31.8 MPa, again showing large variations.

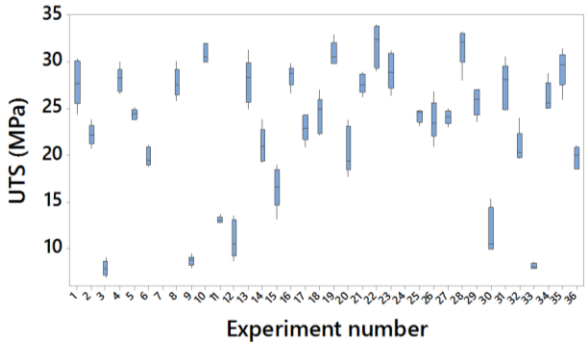

Figure 2.3 Boxplot of UTS grouped in batches

Finally, the same process was followed for the ultimate percent strain (%), and the results are shown in Figure 2.4. All tested samples failed between 2.3% and 10.4% strain; as is represented in Figure 2.4.

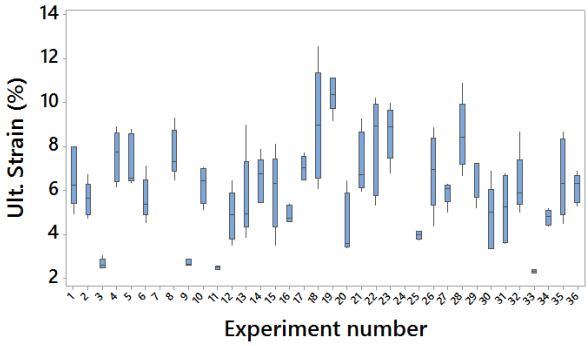

Figure 2.4 Boxplot of Ultimate Strain grouped in batches

2.3.2. Factor analysis

Elastic modulus: the signal to noise ratio (S/N ratio) is a measure to identify the effect of each controllable parameter on the response. Table 2.2 is the output obtained from Minitab under the Taguchi Analysis using "larger is better" configuration on the elastic modulus. In this table, the factors follow the same order as in Table 2.1. Each number is the actual signal to noise ratio for each level of each factor on the elastic modulus. "Delta" designates the difference between the maximum and minimum values of S/N ratio for each level of each factor. The rank is the position of each factor in a relevance scale for the desired output; in this case, factor number 4 is the most relevant factor and corresponds to *layer thickness*.

Table 2.2 S/N ratio response for elastic modulus (Larger is better)

	Factor Number (refer to Table 2.1)											
Level	1	2	3	4	5	6	7	8	9	10	11	12
1	-2.661	-1.856	-2.218	0.426	-1.089	-2.543	-2.28	-1.942	-2.2	-2.035	-1.728	-2.584
2	-1.439	-2.222	-1.861	-1.659	-2.113	-2.462	-1.678	-1.555	-1.961	-1.646	-2.458	-1.415
3	-	-	-	-4.953	-2.788	-1.221	-2.171	-2.604	-1.975	-2.506	-1.947	-2.209
Delta	1.222	0.365	0.357	5.379	1.698	1.321	0.601	1.049	0.239	0.860	0.729	1.168
Rank	4	10	11	1	2	3	9	6	12	7	8	5

Following the rank order, the factor number 4 on its own is responsible of the 35% of the elastic modulus variation; and the 3 most important factors (4, 5 and 6) account for the 56% of the response variation, while factors 4, 5, 6 and 1 (the 4th highest ranked) account for the 64% of the response.

Figure 2.5 shows the mean elastic modulus results for each level and factor. The most significant change is observed for different *layer thickness* values, varying from 1.06 GPa for 10 µm layers to 0.56 GPa for 50 µm layers, almost a 50% decrease in elastic modulus.

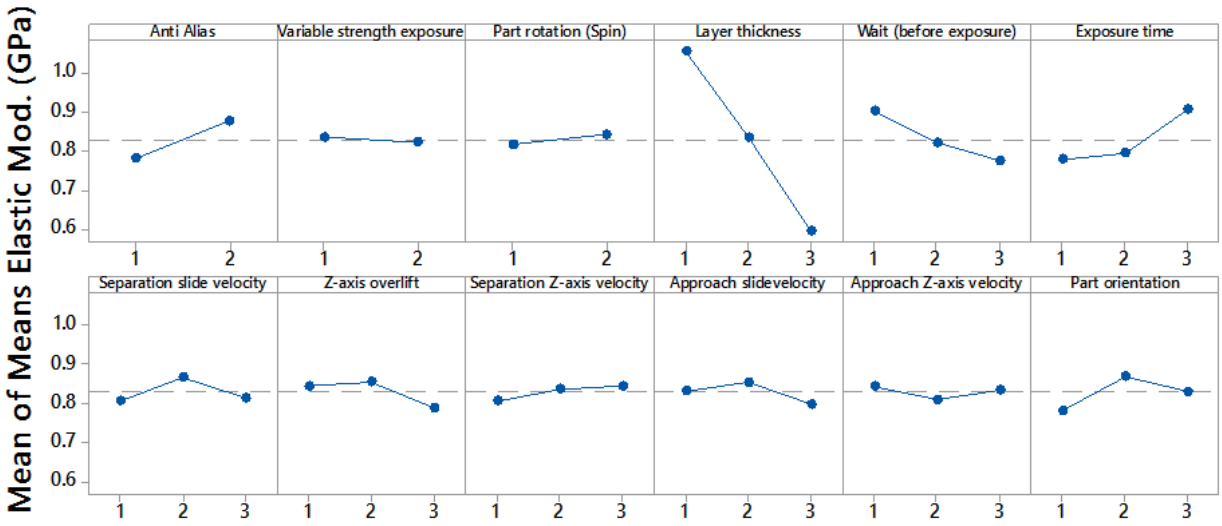

Figure 2.5 Main effect mean of elastic modulus' means

Ultimate tensile strength: Table 2.3 shows the results of the Taguchi Analysis for UTS.

Table 2.3 S/N ratio for UTS (Larger is better)

	Factor Number (refer to Table 2.1)											
Level	1	2	3	4	5	6	7	8	9	10	11	12
1	25.87	26.9	26.02	29.08	27.94	25.97	26.66	26.5	26.24	26.8	26.77	26.59
2	27.21	26.22	27.13	27.16	26.36	26.2	26.5	27.22	26.62	27.07	26.15	27.88
3	-	-	-	23.32	25.55	27.38	26.46	25.96	26.8	25.7	26.73	25.03
Delta	1.34	0.68	1.11	5.76	2.39	1.42	0.2	1.27	0.56	1.37	0.61	2.86
Rank	6	9	8	1	3	4	12	7	11	5	10	2

It must be noted that the top three factors (4, 12 and 5) are different from those found for the elastic modulus, meaning that factors affect in different manners to each mechanical property. These factors account for a 56% variation of the response.

The mean values of UTS for each factor and level are represented in Figure 2.6. The variations on the *layer thickness* introduce the largest variations on the UTS mean, varying in the range of

16.4 MPa for 50 µm to 28.7 MPa for 10 µm *layer thickness*. The *part orientation* introduces significant differences too, varying from an average of 22.7 MPa for the X orientation to 25.4 MPa for the Y orientation and 20.1 for the Z direction, which involves a 21% reduction of UTS.

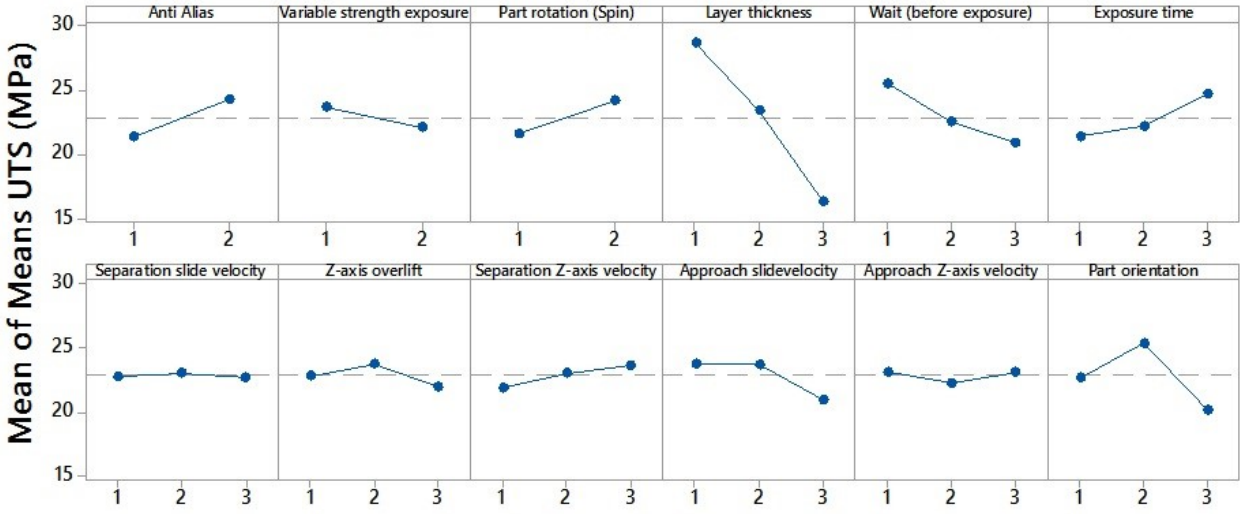

Figure 2.6 Main effect Mean of UTS' Means

Ultimate strain: Following the same steps as for the elastic modulus and UTS, the ultimate strain results are studied. The most relevant factors in the rank shown in Table 4 are 12, 4 and 5. These cumulatively represent a 51% of the response variation.

Table 2.4 S/N ratio for ultimate strain (Larger is better)

	Factor Number (refer to Table 2.1)											
Level	1	2	3	4	5	6	7	8	9	10	11	12
1	14.4	15.19	13.86	15.61	16.18	14.55	15.23	14.34	14.2	15.44	14.47	15.52
2	15.09	14.35	15.74	15.34	14.48	14.56	14.37	15	14.92	15.06	14.87	16.42
3	-	-	-	13.22	13.81	15.08	14.59	14.88	15.16	13.7	14.93	12.14
Delta	0.69	0.84	1.88	2.39	2.38	0.53	0.86	0.66	0.96	1.74	0.46	4.28
Rank	9	8	4	2	3	11	7	10	6	5	12	1

Figure 2.7 represents the mean ultimate strain obtained for each used factor at different levels. This time, the highest mean value variation is from 7.1% for Y orientation and 4.6% for Z orientation or, what is the same, a 35% decrease between Y and Z orientations.

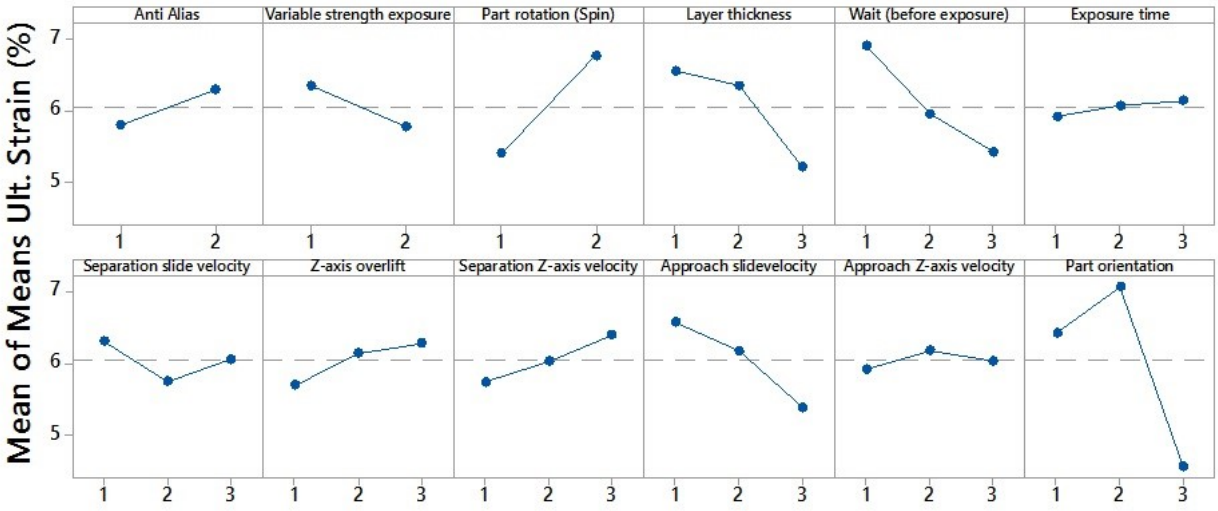

Figure 2.7 Main effect Mean of Ultimate Strain's Means

2.3.3. Cost and time

Different printing parameters result in different printing times which may vary (See Figure 2.8) from minutes to hours. Printing time is an important criterion and contributes directly to the manufacturing cost (which includes machine use, energy, and the like). Design engineers usually carry out wither a stiffness or strength critical design. Although both are equally important, in this paper we highlight the relationship between UTS and print time as a case study for optimized cost analysis. The relationship between elastic modulus and strain versus time can be outlined similarly; however, it is omitted for the sake of brevity.

As seen in Figure 2.8, long print times are not directly related to higher UTS. Specimens printed in less than 30 minutes show a wide range of UTS; demonstrating that for the right combination of factors, UTS can be maximized while the printing time and costs are minimized. As an example, the two sample points encircled using red dots give very similar UTS; however, one can be printed at ~1/10th of the print time taken by the other.

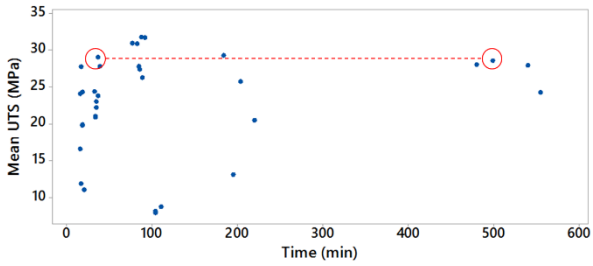

Figure 2.8 Scatterplot of UTS Mean vs. Time

2.3.4. Print setting for optimized model

Following the data analysis, the statistical optimization was carried out based on Taguchi's orthogonal arrays. Table 2.5 highlights the optimized factors obtained for the combined statistical optimization of UTS, elastic modulus and strain. The last two columns presented in Table 2.5 correspond to the optimized level settings and their values, respectively.

Table 2.5 Optimized levels for all mechanical properties

Factor	Factor Name	Unit	Level	Value
1	Anti-Alias	-	2	No
2	Variable strength exposure	-	1	Yes
3	Part rotation (Spin)	-	2	Y axis
4	Layer thickness	µm	1	10
5	Wait (before exposure)	s	1	1.125
6	Exposure time	s	3	2
7	Separation slide velocity	rpm	1	6
8	Z-axis overlift	mm	2	0.75
9	Separation Z-axis velocity	mm/s	3	1.875
10	Approach slide velocity	rpm	1	9
11	Approach Z-axis velocity	mm/s	3	1.875
12	Part orientation	-	2	Y axis

Using the optimized settings, five specimens were printed and tested. The average results were: 1.28 GPa for the elastic modulus, 34 MPa for UTS and 7.4% for the ultimate tensile strain. The

optimized value was higher than the maximum value obtained via DoE (1.25 GPa) as seen in Figure 2.2. The UTS value was on par with the maximum value found using DoE (Figure 2.3). However, the ultimate strain value of the optimized model was found to be approximately in the middle of the findings obtained using DoE (Figure 2.4). Since the optimization used was selected to maximize all the factors (i.e. UTS, elastic modulus and strain), as UTS and elastic modulus increase, one naturally expects a decrease in the maximum strain; therefore, the result obtained for strain is reasonable.

It should be noted, that the optimum levels of each factor do not match the manufacturer recommended values for the given layer thickness (10 μm). The logical reason behind this finding is that the default values will lead to a higher success rate of the printing process than the ones obtained in this study.

2.3.5. Post cured optimized model

After obtaining the results for the best specimen, it was determined that post curing of the specimens keeping them under UV light after printing could be beneficial to increase the obtained mechanical properties.

Five specimens were tested; two of them were post cured for 1 hour and the other three for 2 hours. The results are shown in Table 2.6.

Table 2.6 Ember summary of results for optimized print

Post curing time	Elastic modulus (Gpa)	UTS (Mpa)	Ultimate strain(%)
0 hours	1.3	34	7.4
1hour	2.2	49	4.4
2hours	2.1	45	4.2

One of the most outstanding results is that after 2 hours post curing the mechanical properties are slightly lower than after post curing only for 1 hour. The material becomes more brittle, the dog bone breaks earlier and the elastic modulus decreases. If the comparison is made between the non-post cured specimen and the post cured ones, the elastic modulus almost doubles its value and the UTS increases a 44% (from 34 MPa to 49 MPa). On the other hand, the ultimate strain decreases a 40% (from 7.4% to 4.4%).

2.3.6. Discussion

The results of the study highlight the parameters that affect mechanical properties considered. Variations in parameters manifested 214% increase in UTS, 301% increase in E, 347% increase in strain. Among the investigated parameters, *layer thickness, exposure time*, and *part orientation* were identified as the key parameters with a significant influence on the properties.

Layer thickness: It was determined that a decrease in *layer thickness* leads to an increase in the elastic modulus, UTS, and strain values. This can be attributed to the light transmittance through the layers that decreases exponentially with the depth. It is possible that when a thinner layer is being cured, the light passes beyond that layer and further cures the previous layers causing a continuous increase in the degree of cure, i.e. higher number of covalent bonds, in the overall specimen. Naturally, this effect happens more when using small layer thicknesses. On the contrary, when the layers are thicker, the degree of polymerization is high on the surface of the layer but low on the other end of the layer, causing a weaker connection between layers.

Exposure time: A small increase in *exposure time* leads to an increase in the elastic modulus, UTS, and strain values. Higher *exposure time* allows an increase in the degree of polymerization on every layer. Following the argument presented for the *layer thickness*, the time increase will increase the polymerization degree on all the layer, however, if the full polymerization is not achieved the bottom part of each layer will still show lower mechanical properties. This would weaken the full printed part. However, it should be noted that benefiting the advantages of exposure time is limited by the fact that increasing the time beyond Level 3 poses risk of the layers sticking to the tray. On the other hand, if post curing was added to the specimens, the disadvantages of printing with low exposure times and high layer thickness could be minimized.

Part Orientation: In general, it is observed that *part orientation* has a large effect on properties. Parts printed along the z-axis demonstrated lower properties. One potential explanation is that the adhesion forces between layers is not as resistant as the material itself, producing early failures when the forces are applied perpendicularly to the layer plane. Again, these adhesion forces are related to the polymerization degree mentioned during the explanation of the *layer thickness's* and *exposure time's* effect.

2.4. CONCLUSIONS

In this paper, we report the findings on the effect of Vat-photopolymerization print parameters on elastic modulus, UTS, tensile strain and printing time. It was found that the most significant parameters are *layer thickness*, *part orientation*, and *exposure time*. The thinnest *layer thickness* (10 μm versus 50 μm) has been proved to improve the performance of all the mechanical properties studied. Long *exposure time* improved the elastic modulus, UTS, and ultimate strain. *Part print orientation* showed significant effects on the elastic modulus, UTS, and the ultimate strain. The best results are found for X and Y orientations. A combined statistical optimization based on Taguchi's DoE was utilized to identify the optimized print parameters. The experimental verification of the optimized print parameters was undertaken. Results showed good agreement with the predictions. Finally, print time versus properties were investigated outlining the importance of the optimization process for industrial uses of the machine. Findings will enable design engineers to better tailor their designs according to design specifications.

CHAPTER 3 TENSILE CONSIDERATIONS ON STEREOLITHOGRAPHY VAT-PHOTOPOLYMERIZATION(*)

(*) A version of this chapter is intended to be submitted to Rapid Prototyping Journal as a journal paper with the authors: Elisa Aznarte García, Cagri Ayranci, A.J. Qureshi

3.1. INTRODUCTION

Additive Manufacturing (AM) is a technology that builds parts by material addition rather than material removal as in classical manufacturing processes. First a three-dimensional object is created in a Computer Aided Design (CAD) software, and saved as an STL file. The STL file is sliced and then read by the AM machine to create the printed part by, layer-by-layer, depositing material until the desired shape is achieved. The recent success of desktop-type machines has made AM a successful technology many applications, including for jewelry or decorative purposes; however, adaptation of the technology for broader fields and more complicated applications is still lacking. One of the major bottlenecks in this aspect is availability of data on the effect of print parameters on mechanical properties. There are many factors that affect these properties; Letcher et al. classifies them in vendor related and user related factors. At the same time they are grouped in material properties, printer type, printing parameters defined by the user and geometrical complexity of the part [13].

Stereolithography (SLA) printing uses photosensitive resin to create 3D printed parts by curing layer over layer by the means of a UV light. The machine used in this study uses a single laser beam to polymerize layers of the mentioned resin. There are currently several studies focused on fused deposition modelling (FDM) type of 3D printing but there is not much information on how different printing parameters or conditions affect the final mechanical properties of SLA printed parts. Formlabs® offers one of the few technical information on these types of machines in the form of a series of white papers on mechanical properties, studying separately post curing effect and printing direction [14], [15]. Other studies on FDM and SLA show a clear relationship between the tensile properties and the printing orientation, confirming the high anisotropy of these parts [16]–[19].

This paper studies the relationship between printing factors, post curing and the final tensile properties of parts printed using Formlabs' Clear resin and the Form2 printer. This study also

aims to find the optimal printing procedure to obtain best mechanical properties investing the minimum possible time, hence reducing manufacturing costs.

3.2. MATERIALS AND METHODOLOGY

With the objective stated above, the methodology used is divided into following steps: planning and Design of Experiments (DoE). The DoE was based on knowledge obtained during previous printing experience and pilot experiments to assess the limitations of the printer, testing machine and material. Later, printing as per the designed experiments, tensile testing of the dog bone shaped specimens, and, lastly, analysis of the tensile test results to determine the effect of the studied factors and proposal of an optimized mode of printing.

3.2.1. Equipment

Printer: the printer selected for this study is the Formlabs' Form2. This is a desktop SLA 3D printer with a 250mW laser. According to the manufacturer, the maximum resolution along the printing surface is 140 μm, given by the width of the laser beam. The Z resolution, given by the *layer thickness*, ranges between 25 and 100 μm. The printing envelope is 145x145x175mm (X,Y,Z). The printer's firmware version during the duration of the study was rc-1.9.9-43. The resin used was Formlabs standard clear resin.

CAD software: All CAD models were created using SOLIDWORKS® 2015 by Dassault Systèmes.

Slicing software: the manufacturer's software, PreForm 2.11.3, was used to create the printing files.

Data analysis software: MATLAB R2016a and Minitab® 17.3.1 were used to analyze the experimental data. Osm-Classic was used to track the tensile strain during the elastic region of the stress-strain curve [20].

Universal Testing Machine: A Bose ElectroForce 3200 Test Instrument was used to perform the tensile tests. The machine was equipped with a 450 N capacity load cell.

Camera: the Basler acA3800-10gm camera was used to record the elastic part of the tensile tests.

3.2.2. Methodology

The Form2 printer was used in standard mode, in which the only available parameter to modify at the software level was the *layer thickness*; which could be chosen to be 25, 50 or 100 µm. Additionally, *post curing time*, *part orientation*, *part rotation* and *part position* are factors considered for this experiment.

Part rotation is considered as a 2-level factor as shown in Figure 3.1 (a); *part orientation* and *part position* are a 3-level factor as seen in Figure 3.1 (a) and (b) respectively. Finally, *post curing time* is a 3-level factor, being these 0, 60 and 120 minutes. The post curing process uses a 365 nm wavelength lamp with a measured power of 0.068 W/ cm^2.

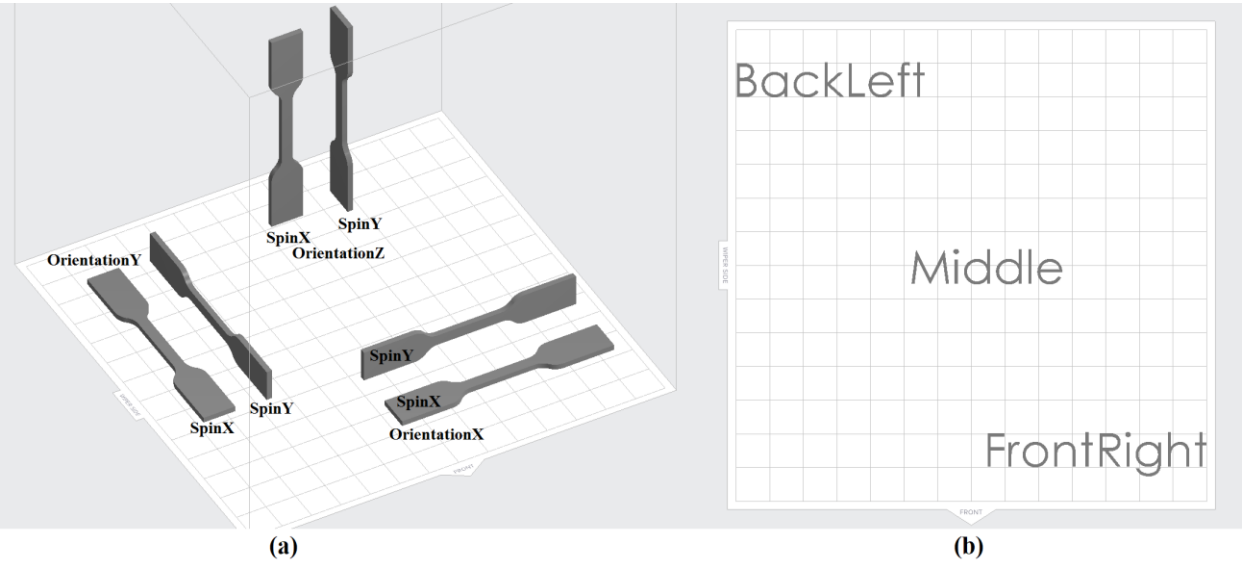

Figure 3.1 (a) Building surface, part orientation and part rotation levels, (b) Part position

3.2.2.1. Design of Experiments

Taguchi's mixed level DoE was implemented using Minitab. Taguchi allows the study of the effect on the response of all the factors keeping the number of experiments to a minimum by the use of an orthogonal array [9], [21]. An L18 array matrix was designed to obtain the 18 different experiments. A total of five replications were run for each experiment; resulting in 90 runs. All 5 samples of each experiment were printed at the same time to establish the mechanical repeatability of a single print.

Taguchi design of experiment is a widely used tool for experimental analysis of processes sensitive to noise coming from different experimental parameters. Its main goal is to minimize the required number of experiments necessary to characterize a process. Taguchi's method was implemented on this study.

Five factors were analyzed on this experiment with 4 being 3-level and one a 2-level factor and the rest of them 3-level factors. Table 3.1 summarizes the factors and levels studied.

Table 3.1 Factors implemented in Taguchi design of experiments

Factor number	Factor Name	Unit	Number of Levels	Level 1	Level 2	Level 3
1	Part rotation (spin)	-	2	X	Y	-
2	Layer thickness	µm	3	25	50	100
3	Part orientation	-	3	X	Y	Z
4	Post curing time	min	3	0	60	120
5	Position	-	3	BackLeft	Middle	FrontRight

Factor 1, **part rotation (spin)**, refers to the rotation of the part with respect to its longitudinal axis; it can be observed in Figure 3.1. *Factor 2*, **layer thickness,** refers to the height variation of the building platform between consecutive layers. *Factor 3*, **part orientation**, refers to the alignment of the part with respect to the axis of the printer as shown in Figure 3.1. *Factor 4*, **post curing time**, indicates the amount of time that the part will be cured under UV light at 60 degrees. *Factor 5*, **position**, indicates the location on the printing surface where the part is printed; which, if the printing process is consistent should not affect in a high manner the final results.

3.2.2.2. Test Specimens

The tensile test specimens used for this work were printed in accordance with the ISO-527-1/2:2012 standard [12]. The maximum break load of the machine used was the limitation taken to choose the test specimen type; which was chosen as ISO527:Type 5B. A schematic view and the dimensions of the specimen are shown in

Figure 3.2.

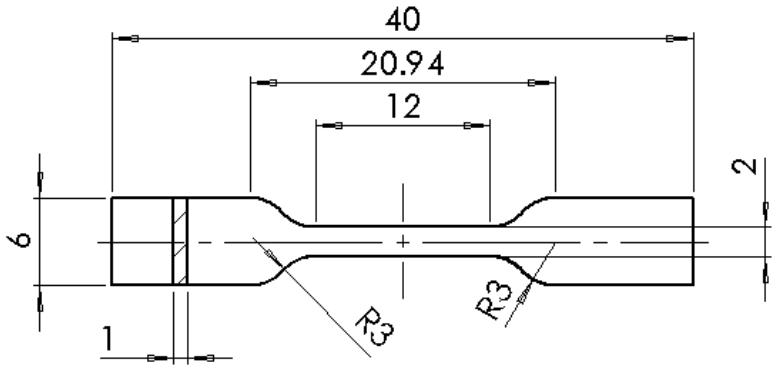

Figure 3.2 ISO 527 specimen type 5B and measurements (mm)

3.2.2.3. Pre-processing

The designed dog bone's CAD file was saved in STL format with a maximum deviation tolerance of 0.002 mm and maximum angle tolerance of 0.5°. The STL file was then opened and processed in PreForm, adding support structure and applying any design constriction required by each experiment. After this process, each unique file is sent to the printer.

3.2.2.4. Post processing

All printed parts are cleaned by immersion in a 99.5% isopropyl alcohol bath for 10 minutes as recommended by the manufacturer. Any existing support structure is removed by the use of pliers and post cured under UV light for the required time at 60°C. The pieces are then left on shelf at room temperature for 24 hours.

3.2.2.5. Tensile testing

Tensile tests and data analysis were performed as per ISO 527:2012 standard [12].

3.3. RESULTS AND DISCUSSION

This section presents the results obtained from the tensile tests experiments. The results have been divided into elastic modulus, ultimate tensile stress (UTS) and ultimate strain measured at the point of break. First, an overall view of all the experiments is shown. Later, the effect of each factor is statistically analyzed individually and ranked in terms of S/N ratio and means response.

To finalize, a brief discussion on the printing time with respect to the mechanical properties is presented as well as a discussion on the findings for each factor.

3.3.1. General interpretation of the results

The boxplot of the elastic modulus obtained for all the experiments is shown in Figure 3.3; on which the blue bars are the range between the first and third quartile and the black lines represent the minimum and maximum values. Each bar represents the 5 results corresponding to 5 repetitions of the same experiment; each experiment has a unique combination of factors as per Taguchi's design. The average of each batch varies between 3.08 GPa and 0.97 GPa, representing a 216% increment on the elastic modulus for the same material printed under different conditions. However, the mentioned variation is with respect to the averages of each experiment, the maximum elastic modulus was reported to be 4.10 GPa while the minimum was 0.93 GPa, increasing the difference to a 342%. This change reported in the difference of results when comparing averages or individual elastic moduli is due to the high-observed standard deviation, especially for the post cured samples.

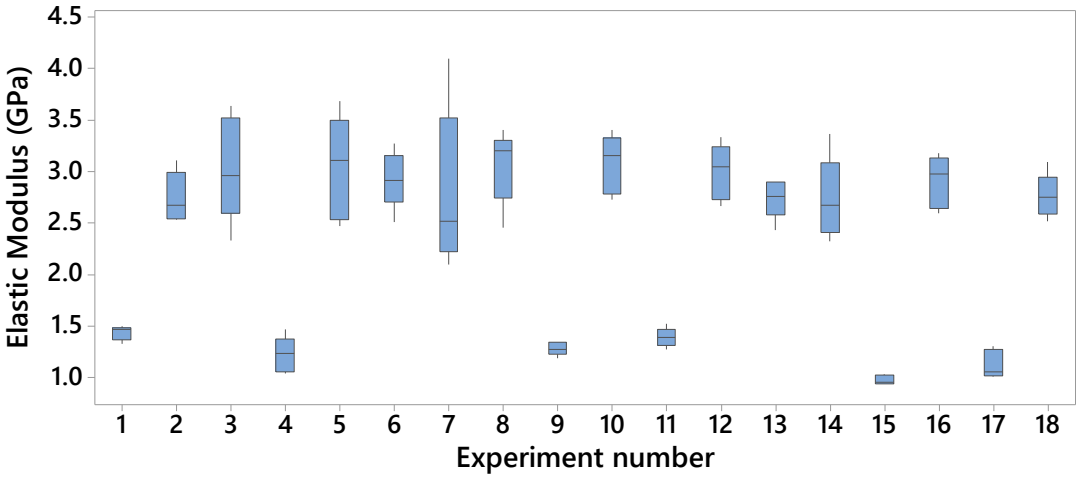

Figure 3.3 Boxplot of elastic moduli grouped in batches

Similarly, the boxplot of the test samples' ultimate tensile strength (UTS) is observed in Figure 3.4. The mean UTS values vary between 63.8 MPa and 28.6 MPa; showing again a 123% difference between the minimum and maximum values on average of each batch and 181% when comparing global maximum and minimum individual results (24.3 MPa and 68.5 MPa respectively). This time, the standard deviation is reported to be lower, hence the difference

when comparing global maximum and minimum values and maximum and minimum averages is lower.

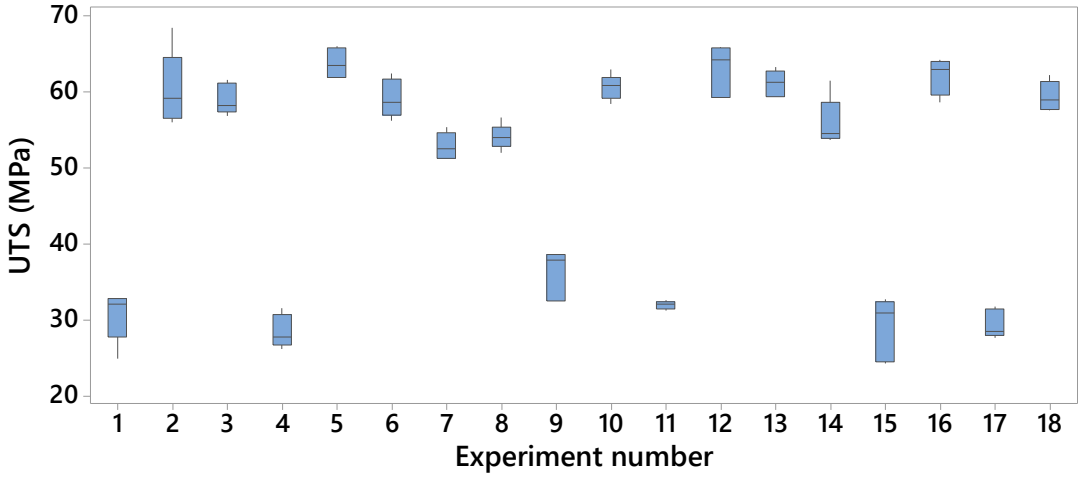

Figure 3.4 Boxplot of UTS grouped in batches

Finally, the same method was used for the ultimate strain expressed as a percentage (%). The corresponding boxplot can be observed in Figure 3.5. In average, all experiments failed between 11 % and 44 % strain, representing an increment of 314%; whereas the global minimum ultimate strain was reported to be 6% and maximum ultimate strain was 49%, meaning that the specimen that broke at the highest ultimate strain overcame more than 7 times more strain than the one that broke with minimum strain.

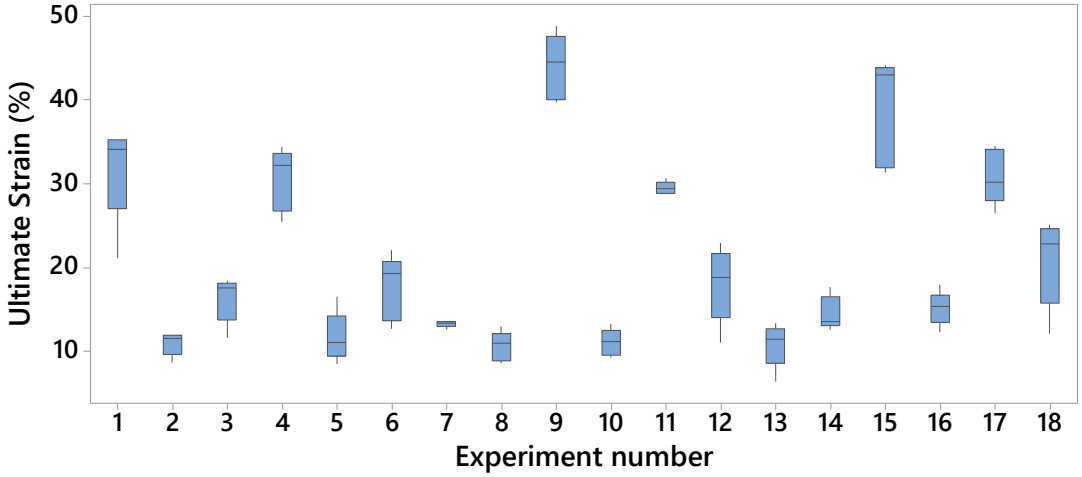

Figure 3.5 Boxplot of ultimate strain grouped in batches

3.3.2. Factor analysis by response

Elastic modulus: the main output from a Taguchi analysis is the Signal to Noise ratio (S/N ratio). This magnitude measures the effect of each factor included in the DoE. To calculate the S/N ratio a given configuration must be chosen, depending on the desired output; In this case, "larger is better" was used. Table 3.2 shows the results of the analysis.

The numbers observed are the S/N ratio for all levels of each factor. Delta represents the S/N ratio variation within the same factor, calculated as maximum S/N ratio minus minimum S/N ratio. Rank shows the order of the factors in terms of largest Delta. In this case, *post curing time* is the most relevant factor that will affect the resulting elastic modulus.

Table 3.2 S/N ratio response for elastic modulus (Larger is better)

Level	Spin	Layer thickness	Orientation	Post curing time	Position
1	6.797	7.174	6.738	1.688	6.784
2	6.414	6.174	6.635	8.88	6.352
3	-	6.469	6.444	9.249	6.681
Delta	0.383	1	0.294	7.561	0.432
Rank	4	2	5	1	3

An evaluation of the delta values shows that the first ranked factor, *post curing time*, accounts for the 78% of the elastic modulus variation. The next ranked factor, *layer thickness*, is only responsible for the 10% of the response. All other factors represent, individually, less than a 5% of the response.

Finally, Figure 3.6 represents the Plot of Means of the elastic modulus of each individual level. From all the 90 experiments, the average elastic modulus of those that were post cured for 2 hours was 2.96 GPa; while those samples that were not post cured had an average value of 1.24 GPa. It is observed that the elastic modulus results did not undergo a relevant variation when varying other factors.

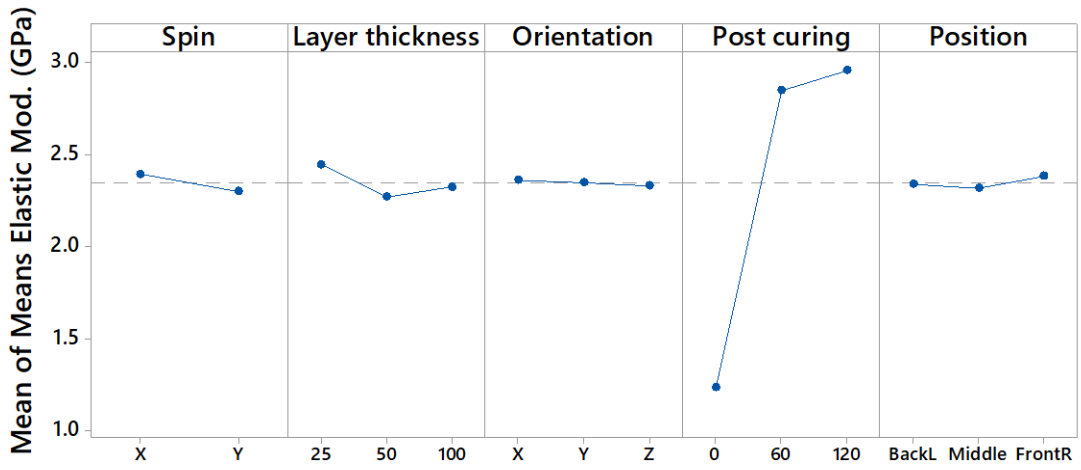

Figure 3.6 Main effect mean of elastic modulus' means

Ultimate tensile strength: the same steps were followed to analyze the ultimate tensile strength (UTS) results. The S/N ratio results are found in Table 3.3. Again, the top ranked factor is *post curing time*; however, the second most important factor is part *position* instead of the *layer thickness*. This change indicates that not every factor affects different mechanical properties in the same manner. This time, *post curing time* represents an 82% of the variation in UTS.

Table 3.3 S/N ratio for UTS (Larger is better)

Level	Spin	Layer thickness	Orientation	Post curing time	Position
1	33.47	33.7	33.38	29.69	33.32
2	33.55	33.37	33.44	35.53	33.34
3	-	33.47	33.72	35.31	33.88
Delta	0.08	0.33	0.34	5.84	0.55
Rank	5	4	3	1	2

The mean UTS values can be found in Figure 3.7. The most significant differences are introduced by the different *post curing time* levels, in this case, the mean UTS ranges between 60.0 MPa for one hour post curing and 31 MPa for no post curing.

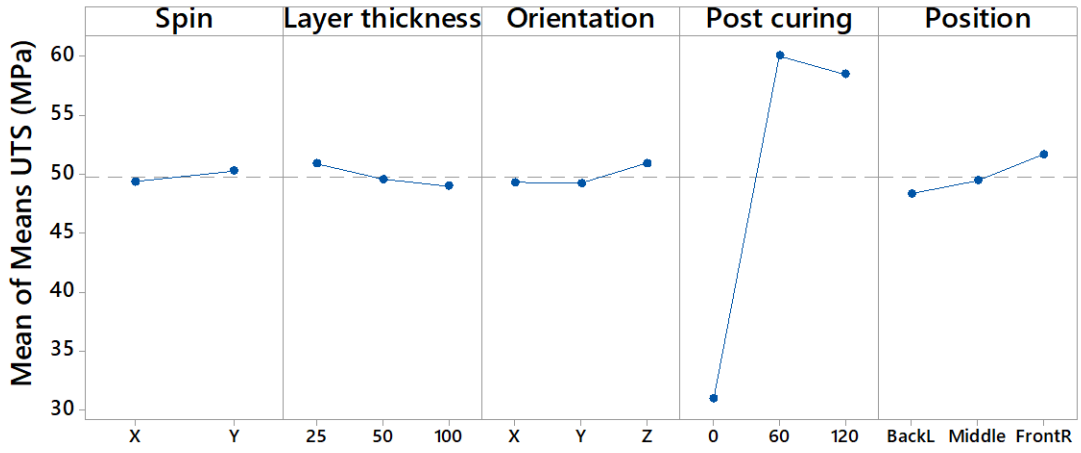

Figure 3.7 Main effect mean of UTS' means

Ultimate strain: following the same analysis procedure as above, the ultimate tensile strain is studied. The highest ranked factor is, one more time, the *post curing time*, that represents a 60% of the response variation, followed by the *part orientation* representing a 22%. The signal to noise ratio values can be observed in Table 3.4.

Table 3.4 S/N ratio for ultimate strain (Larger is better)

Level	Spin	Layer thickness	Orientation	Post curing time	Position
1	24.88	24.68	24.2	30.39	25.67
2	25.21	24.82	23.94	22.17	24.91
3	-	25.64	27	22.58	24.56
Delta	0.33	0.96	3.06	8.22	1.11
Rank	5	4	2	1	3

The mean ultimate strain is represented in Figure 3.8. Opposed to the previous results, this time the highest response is given for no post cured samples while post cured specimens show the lowest strain values (34% ultimate strain compared to 14%).

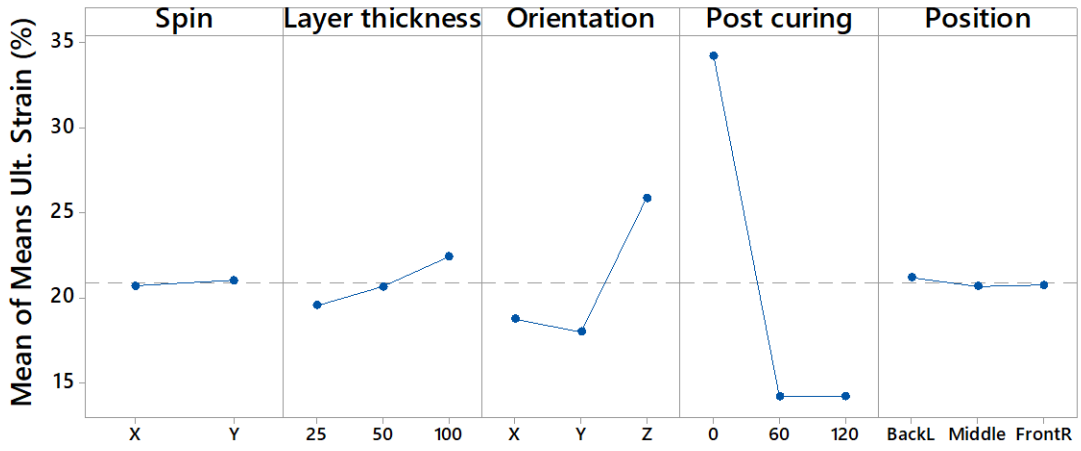

Figure 3.8 Main effect mean of ultimate strain's means

3.3.3. Cost and time

The printing time for each of the designed experiments is a function of the *part orientation*, and other manufacturing process parameters. Therefore, each of the considered experiments results into a different print time. Printed parts also require post processing, so, post processing time should be added to the printing time. For this analysis, the sum of the estimated print time given by the software and the *post curing time* was used. Figure 3.9 shows the average UTS of each experiment with respect to the total time. It is important to mention that the manufacturing cost is directly related to time in terms of machine use and energy. Labor time will remain approximately constant for any 3D printed part if no intervention is necessary by the operator. However, there is an increased probability of requirement of operator intervention as the print time increases.

As observed in Figure 3.9, similar UTS results can be obtained from samples that take around 2 hours and 5 hours to print, with the latter being more than two times more expensive in terms of manufacturing time. On the figure, each point represents one of the 18 experiments that were run. This study highlights that combinations of factors that lead to long manufacturing time should not be blindly associated with the obtainment of better UTS results. Additionally, too short manufacturing times, below 100 minutes corresponding to non-post cured parts, show about half UTS (30 MPa) than the average post cured samples (60MPa).

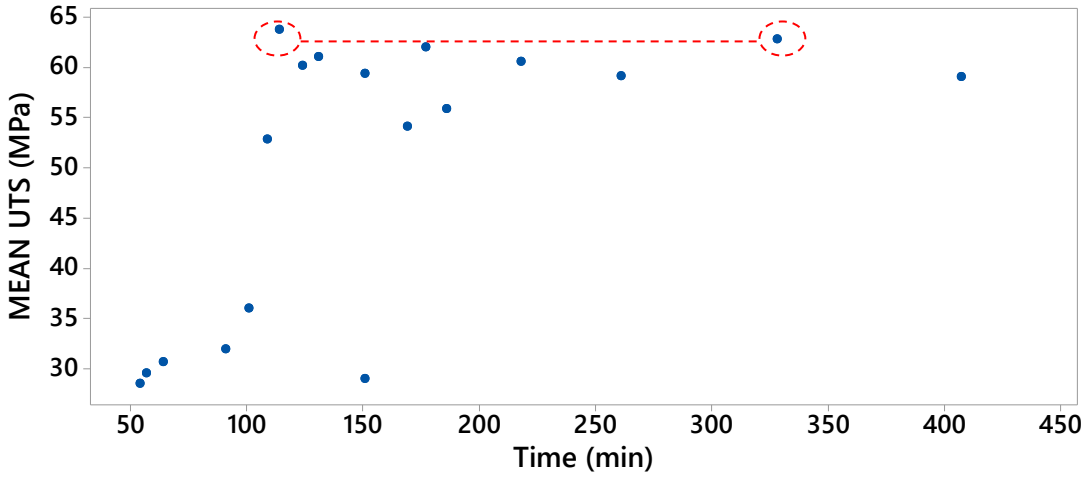

Figure 3.9 Scatterplot of UTS mean vs. time

3.3.4. Print settings for optimized model

To conclude the design of the experiments the optimized print settings were extracted for the different mechanical properties studied.

Firstly, the individual and combined optimizations were obtained for both elastic modulus and UTS. Resulting in 3 experiments where the most influencing factors were constant, hence the optimized elastic modulus configuration was chosen for testing.

Table 3.5 highlights the optimized experiment for highest resulting elastic modulus. The optimized theoretical value of this test is an elastic modulus of 3.1 GPa, UTS of 57.1 MPa and ultimate strain of 10.88%.

Table 3.5 Optimized levels for elastic modulus

Factor	Factor Name	Unit	Level	Value
1	Part rotation (spin)	-	1	X
2	Layer thickness	µm	1	25
3	Part orientation	-	1	X
4	Post curing time	min	3	120
5	Position	-	1	BackL

After the experiment was run, the resulting average elastic modulus was 2.99 GPa, UTS 54.5 MPa and ultimate strain 15.3%. This result validates the optimization being the obtained elastic

modulus and UTS within a 5% of the predicted ones. The ultimate strain ended up being larger than expected.

To continue the statistical optimization, the experiment with highest ultimate strain was designed and estimated. Table 3.6 shows the optimal combination of parameters for the given factors. The estimated ultimate strain is 41%, with an elastic modulus of 1.14 GPa and an UTS of 30.2 MPa.

Table 3.6 Optimized levels for ultimate strain

Factor	Factor Name	Unit	Level	Value
1	Part rotation (spin)	-	2	Y
2	Layer thickness	µm	3	100
3	Part orientation	-	3	Z
4	Post curing time	min	1	0
5	Position	-	1	BackL

The tested samples ended up breaking before reaching the expected strain, exactly at an average of 28% strain with a high standard deviation of 7.6%. However, it must be noted that this average is the result of 3 tensile tests, being the ultimate strains 22, 25 and 36%. If the highest of these numbers is compared with the tests performed, only two of the eighteen experiments have higher ultimate strains. The origin of this high variability in the results can come from uncontrollable factors like ambient humidity or defects on the surface lest by the support tip.The elastic modulus and UTS were closer to the predicted values, 1.3 GPa and 29.4 MPa respectively.

3.3.5. Discussion

The experimental results and statistical analysis provide critical insight in the effect of process factors on the mechanical properties of the printed parts. The Taguchi's design of experiment ranks the factors and it shows that *post curing time* is the most important factor that affects the mechanical properties. *Post curing time* is a post printing factor, meaning that it is introduced during the post processing stage. In terms of factor significance within the printing process itself, the *part orientation* is the most significant factor, followed by the *layer thickness*, part *position*, and finally, *part spin*. This order of factors was obtained adding the percentage effect of each factor over the three mechanical properties studied.

Post curing time: it was shown that post curing the tensile specimens increases the elastic modulus and UTS by 2 or 3 times, being this increase of similar magnitude for only 1 hour of post curing or 2 hours. On the other hand, post curing decreases the ultimate tensile strain. It is possible that the effect of *post curing time* was intensified due to the small size of the specimens, making it possible for the UV light to go through the full part reaching the interior of the dog bones. The fact that post cured specimens show higher elastic modulus and UTS is directly related to the polymerization degree of the resin.

Part orientation: the analysis of the results shows that the part orientation significantly affects the ultimate tensile strain. This effect is significantly higher on parts printed along the Z-axis. It is possible that the bond at the interface of the previous layer and the current layer being exposed is more ductile than the bond within the exposure layer itself; delaying the breaking point by avoiding the premature brittle failure of the layers themselves.

Layer thickness: decreasing the *layer thickness* is related to an increase of the resulting elastic modulus and UTS. This can be due to the transmittance of UV light trough the layers; thinner layers allow more previous layers to be cured further, including the gap between layers and leading to a higher polymerization degree. On the contrary, thicker layers lead to higher ultimate strain percentages. However, the effect is very small compared to *post curing time*. Other aspects, as its effect on printing time, could become more important than its effect on the mechanical properties when post curing of the specimens is performed.

In order to further study the *layer thickness* effect on non-post cured samples, four more experiments were prepared and tested. The only factors accounted for were *layer thickness* and *part orientation*, that were assigned the values corresponding to levels 1 and 3. Those that were printed along the z direction were proven to have better mechanical properties; with an elastic modulus of 1.4 GPa opposed to 0.9 GPa; a UTS of 38 MPa against 28 MPa; and an ultimate strain of 38% versus 34%. Likewise, those parts printed with 25 μm thickness layers also showed better mechanical properties, except for ultimate strain, than those printed with 100 μm; an elastic modulus of 1.4 GPa and 0.9 GPa, UTS of 37 MPa and 27 MPa but ultimate strain of 31% and 41% respectively.

Part position and part spin: these factors' effect is, again, so low for every response that any *position* or *spin* could be considered without affecting the mechanical properties. The fact that the part *position* has a very low effect is conditioned by the accuracy of the assembly and the low distortion of the optical parts. In addition, the small distances that the laser beam must travel through make the distortions caused by increase in the beam diameter very low. The *spin* on which the part is printed does not cause variations in the mechanical properties because, for any of the chosen parts orientations, the angle between the force during the tensile test and the layers is constant.

3.4. CONCLUSIONS

The effect on the tensile properties on 90 tensile specimens was tested and analyzed. Post processing of these specimens was carefully controlled to minimize the effect of external factors. The results obtained after the analysis and verification of the properties were:

- In general, it can be affirmed that parts printed in clear resin on the Form2 3D printer and post cured during at least 1 hour are isotropic. Its average effect on the mechanical properties was 5.8%.
- Non post cured parts show signs of being orthotropic, though further research should be made to confirm this.
- Post curing highly increases the mechanical performance of the parts, making post curing necessary for any application. The average elastic modulus of non-post cured parts was 1.2 GPa, the UTS was 31 MPa and the ultimate strain was 34%; while the average on post cured parts was 2.9 GPa, 59 MPa and 14% respectively. Post curing after cleaning is also recommended to avoid the stickiness of the parts.
- Long manufacturing times are not related to high elastic modulus or UTS, high mechanical properties can be achieved at low printing times.
- The printing process can be optimized by minimizing the printing time, hence reducing cost and achieving notable mechanical properties.

To support these conclusions, the optimized pieces were printed and tested, obtaining the expected high results in mechanical properties, though given the high standard deviation of the ultimate strain this property could not be predicted as accurately as the elastic modulus and UTS.

To finish, in order to extend the study on not post cured samples, the extra specimens tested showed some trends that confirm that to obtain higher elastic modulus and UTS parts should be printed with the minimum thickness layers and oriented in such manner that the forces applied on the printed part are perpendicular to the layer plane.

CHAPTER 4 DISCUSSION AND FUTURE WORK

This work investigates the printing factors effect on mechanical properties of parts printed via two different vat photopolymerization printers, i.e. Ember and Form 2. In this section, some differences between the two processes analyzed are highlighted. Later, a comparison between similar factors on both printers is shown. To finish, a summary of conclusions and future work are presented.

4.1. TECHNOLOGY DIFFERENCES

Ember and Form2 are AM devices that fall under the vat-photopolymerization classification. However, as explained in chapters 2 and 3, one is DLP and the other one SLA. The main difference is that Ember projects light with a light projector, one full layer at once, while Form2 uses a single laser beam. Both systems have different light power and the curing depth in a single exposure is different. While Ember is an open source printer and the user can adjust every possible parameter, the Form2 does not offer those options. Form2 has an "open mode" available to try third party resins; however, the user cannot modify the pre-defined settings for the company's own resins. This means that if the user intends to use a given resin, he or she will have to find the most similar option among the Formlab's catalogue and use the given settings for that resin.

Of all the factors implemented in the experiments, only *part rotation (spin)*, *layer thickness*, and *part orientation* are common in both studies. The corresponding levels of these factors are constant for part rotation and orientation while *layer thickness* varies between 10, 25 and 50 μm for Ember and 25, 50 and 100 μm for Form2.

Among those factors that are present in only one study, some similarities can be found between *exposure time* (Ember) and *post curing time* (Form2). These two factors affect directly the polymerization rate of the resins, the first one is applied layer-by-layer and the second one is applied during a much longer time to the full piece after the cleaning process. It should be noted that there is a limit on the increment of exposure time in the Ember defined by the time at which the new layers adhere to the PDMS window and the print process cannot continue.

The Ember's factors that are implemented during the printing process are not available or are not controllable in the Form2. In the same manner, Ember's printing surface is so small that the part *position* cannot be considered in a study of this type unless the part size is significantly reduced.

Regarding the *post curing*, there is a noticeable difference between the green parts that come out of the Ember and those printed in the Form2. Parts printed in Ember with the PR-48 resin have a good surface hardness while parts from the Form2 present soft and sticky surfaces, indicating that the polymerization is not complete and curing after printing is necessary.

4.2. COMPARISON OF RESULTS

Given the process differences stated in the previous section, in both cases it was found that the effect of the printing factors on the final mechanical properties is of high importance. Among the common factors present in both studies, *layer thickness* is a main factor for uncured samples. There is always a direct relationship between low layer thicknesses and high mechanical properties. When post curing is introduced, the effect of the *layer thickness* is decreased to a point where its effect becomes insignificant.

The opposite effect happens with the *part orientation*. While in the Ember the lowest mechanical properties are associated to parts printed along the Z direction (layer perpendicular to the applied force during a tensile test), in the case of the Form2, this orientation is related to higher mechanical properties. This difference may be due to the different chemical composition of the resins, probably a lower content of UV blocker that allows the light to travel between consecutive layers; it must be noted that the composition of the Formlabs resin is unknown so this is just speculation.

In general, both materials show improvement in mechanical properties after being post cured. Ember's resin, PR-48 presents much lower properties, breaking in a brittle manner at low strains. Non-post cured Formlabs clear resin have similar elastic modulus and UTS compared to PR-48; however, it can undergo up to 4 times more strain before breaking, making it a more ductile material. Post cured samples from Ember showed better elastic modulus and UTS than non-post cured samples from the Form2 but lower than post cured samples from the Form2. The ultimate strain resulted to be lower than any sample tested from the Formlabs clear resin.

4.3. CONCLUSIONS AND FUTURE WORK

The effect of printing parameters on the tensile properties was studied in this thesis. A summary of the most relevant factors found and their percentage effect on each of the studied responses is shown in Table 4.1; where those factors with an effect higher than 10% are highlighted. Additionally, the optimized levels and values of those factors are included in the last two rows of the table. The calculation of the percentage effect of the factors is done considering the cumulative S/N ratio difference of all the studied factors.

Table 4.1 Summary of factor's effect

			Spin	Layer thickness	Wait before exposure	Part orientation	Post curing time	Position
Elastic modulus	Ember	Rank (out of 12)	11	1	2	5	-	-
		% effect	2.4	35.9	11.3	7.8	-	-
	Form2	Rank (out of 5)	4	2	-	5	1	3
		% effect	4.0	10.3	-	3.0	78.2	4.5
UTS	Ember	Rank (out of 12)	8	1	3	2	-	-
		% effect	5.7	29.4	12.2	14.6	-	-
	Form2	Rank (out of 5)	5	4	-	3	1	2
		% effect	1.1	4.6	-	4.8	81.8	7.7
Ultimate strain	Ember	Rank (out of 12)	4	2	3	1	-	-
		% effect	10.6	13.5	13.5	24.2	-	-
	Form2	Rank (out of 5)	5	4	-	2	1	3
		% effect	2.4	7.0	-	22.4	60.1	8.1
Optimized factors	Ember	Optimized Level	2	1	1	2	-	-
		Optimized Value	Y axis	10 µm	1.125 s	Y axis	-	-
	Form2	Optimized Level	1	1	-	1	3	1
		Optimized Value	X axis	25 µm	-	X axis	120 min	BackL

It was proved that the most important factors are:

- *Part orientation*, especially for the Ember and those cases when the specimens from the Form2 are not post cured. As observed in Table 4.1, it is the factor with the highest effect on the ultimate strain on the Ember and the second most important factor on the Form2.

- *Layer thickness*, that shows a high importance level by the percentage effect on all mechanical properties on the Ember and also, on the elastic modulus of pieces printed with the Form2.
- Curing time, by means of either *exposure time* or *post curing time*. Although it is not shown in Table 4.1, *exposure time* on the Ember is the third and fourth ranked factor on elastic modulus and ultimate stress respectively. With regards to *post curing time* on the Form2, this factor accounts for the majority of the mechanical properties studied, going over an 80% in the ultimate stress response.

Finally, *wait before exposure* goes over a 10% effect on all responses studied.

Findings of this thesis can be used to draw some general conclusions for different vat-photopolymerization processes or machines. *Part orientation* rises as an important factor on these printers, not only using the technology presented on this research, but also on other 3D printing techniques [8], [9], [17], [22], [23]. Additionally, the curing depth of the photosensitive resins related to the relationship (working curve) between the light dose from a given light source and the thickness of the cured layer. The light dose is determined by the time that it is active and the irradiance that is applied. The irradiance decreases exponentially with the depth of the resin [24]; this means that the curing power of the light is higher at the surface of the resin than at the other end of the curing layer. Upon determination of the working curve of the resin being used, the relationship between *layer thickness* and *exposure time* can be established. As the polymerization degree increases, the mechanical properties are also expected to increase on any given set up. Finally, if the set up allows it, the waiting time between the exposure of each layer can be modified accordingly to the trend of the results shown in this thesis.

Some considerations for designers can be extracted from the results of this thesis. It was proven that some factors do not affect in a highly manner the mechanical properties so they can be chosen upon other criteria. However, the *part orientation* and *layer thickness* are implemented by the designer and are critical to the mechanical performance of the parts.

To conclude, the main contributions of this thesis are:

- The quantitative analysis of a wide number of printing factors, physical orientation and post processing factors. Supported by the ranking of their effect on mechanical properties.

- The overall comparison between printing or manufacturing time and UTS. Showing that slow manufacturing processes are not associated to better mechanical properties. Leading to the possibility of optimizing mechanical properties while minimizing cost and time.
- The need of post curing any specimen that will be subjected to several external loads, for example, as part of a mechanism.

The main limitation of this thesis falls in the chemistry of the resins, which was not studied; hence, the results cannot be extrapolated to other resins whose chemical composition differs from the studied ones. This is also a reason why same factors affect the mechanical properties in different manner.

In the near future, this study could be expanded by characterizing the specimens for other failure modes like bending, compression and torsion. These experiments could be run eliminating the factors that have been shown to have less effect on the tensile properties, which may decrease the number of experiments or give more accurate results by adding a higher number of repetitions for each test.

This thesis also shows the basis for an important research path to be continued in the future. A broader study in the degree of monomer conversion and curing kinetics and its effect on the mechanical properties should be performed with respect to the proposed factors on this thesis.

A quantitative analysis of the degree of conversion can be achieved by Fourier Transform Infrared (FTIR) spectrometry. This type of test allows a rapid measurement of the conversion of reactive functional groups of the resin, being the main technique to evaluate the resin curing kinetic. This study should be applied, not only to the green parts as they come out of the printer, also to the post cured samples.

Results of the future work should be compiled and compared to the ones presented in this thesis and could be implemented towards the development of a simulation tool for 3D printed parts. This tool will include: materials, printing settings, orientation and any other factor needed to successfully predict mechanical properties of parts without the need of performing mechanical testing on them.

REFERENCES

[1] K. V Wong and A. Hernandez, "A Review of Additive Manufacturing," *ISRN Mech. Eng.*, vol. 2012, pp. 1–10, 2012.

[2] C. W. Hull, "Apparatus for production of three-dimensional objects by stereolithography," *US Pat. 4,575,330*, pp. 1–16, 1986.

[3] R. Comerford, "A quick look at rapid prototyping," *IEEE Spectr.*, vol. 30, no. 9, pp. 28–29, 1993.

[4] H. Gong, M. Beauchamp, S. Perry, A. T. Woolley, and G. P. Nordin, "Optical approach to resin formulation for 3D printed microfluidics," *RSC Adv.*, vol. 5, no. 129, pp. 3627–3637, 2015.

[5] J. Y. H. Fuh, L. Lu, C. C. Tan, Z. X. Shen, and S. Chew, "Processing and characterising photo-sensitive polymer in the rapid prototyping process," *J. Mater. Process. Technol.*, vol. 89–90, pp. 211–217, 1999.

[6] S. Waheed, J. M. Cabot, N. P. Macdonald, T. Lewis, R. M. Guijt, B. Paull, and M. C. Breadmore, "3D printed microfluidic devices: enablers and barriers," *Lab Chip*, vol. 16, no. 11, pp. 1993–2013, 2016.

[7] G. V. Salmoria, C. H. Ahrens, M. Fredel, V. Soldi, and A. T. N. Pires, "Stereolithography somos 7110 resin: mechanical behavior and fractography of parts post-cured by different methods," *Polym. Test.*, vol. 24, no. 2, pp. 157–162, Apr. 2005.

[8] K. M. Rahman, T. Letcher, and R. Reese, "Mechanical Properties of Additively Manufactured PEEK Components Using Fused Filament Fabrication," in *Volume 2A: Advanced Manufacturing*, 2015, p. V02AT02A009.

[9] A. J. Qureshi, S. Mahmood, W. L. . Wong, and D. Talamona, "Design for Scalability and Strength Optimisation for components created through FDM process," in *Iced 2015*, 2015, no. October, pp. 1–12.

[10] S. Mahmood, D. Talamona, K. L. Goh, and A. J. Qureshi, "Fast deviation simulation for 'Fused Deposition Modeling' process," *14th CIRP Conf. Comput. Aided Tolenracing*, vol.

43, pp. 327–332, 2016.

[11] B. M. Tymrak, M. Kreiger, and J. M. Pearce, “Mechanical properties of components fabricated with open-source 3-D printers under realistic environmental conditions,” *Mater. Des.*, vol. 58, pp. 242–246, 2014.

[12] ISO, “Plastics - Determination of tensile properties - Part2: Test conditions for moulding and extrusion plastics,” *Organization for Standardization*, vol. 2012. International Organization for Standardization, 2012.

[13] T. Letcher, “IMECE2015-52634 EXPERIMENTAL STUDY OF MECHANICAL PROPERTIES OF ADDITIVELY,” pp. 1–8, 2016.

[14] B. Z. Zguris, “How Mechanical Properties of Stereolithography 3D Prints are Affected by UV Curing,” *Formlabs*.

[15] Formlabs, “Validating Isotropy in SLA 3D Printing.”

[16] M. Monzón, Z. Ortega, A. Hernández, R. Paz, and F. Ortega, “Anisotropy of Photopolymer Parts Made by Digital Light Processing,” *Materials (Basel).*, vol. 10, no. 1, p. 64, 2017.

[17] M. Fernandez-Vicente, W. Calle, S. Ferrandiz, and A. Conejero, “Effect of Infill Parameters on Tensile Mechanical Behavior in Desktop 3D Printing,” *3D Print. Addit. Manuf.*, vol. 3, no. 3, pp. 183–192, 2016.

[18] M. Schlepers, “Investigation of the mechanical properties of 3D printed structures of Objet and DLP.,” 2014.

[19] V. O. E. Väyrynen, J. Tanner, and P. K. Vallittu, “The anisotropicity of the flexural properties of an occlusal device material processed by stereolithography,” *J. Prosthet. Dent.*, vol. 116, no. 5, pp. 811–817, 2016.

[20] D. Aldrich, C. Ayranci, and D. Nobes, “Osm-Classic: An optical imaging technique for accurately determining strain,” *SoftwareX*, 2017.

[21] M. S. Phadke, “Quality Engineering using Design of Experiments,” in *Quality Control,*

Robust Design, and the Taguchi Method, Boston, MA: Springer US, 1989, pp. 31–50.

[22] K. Puebla, K. Arcaute, R. Quintana, and R. B. Wicker, "Effects of environmental conditions, aging, and build orientations on the mechanical properties of ASTM type I specimens manufactured via stereolithography," *Rapid Prototyp. J.*, vol. 18, no. 5, pp. 374–388, 2012.

[23] B. E. Carroll, T. A. Palmer, and A. M. Beese, "Anisotropic tensile behavior of Ti-6Al-4V components fabricated with directed energy deposition additive manufacturing," *Acta Mater.*, vol. 87, pp. 309–320, 2015.

[24] K. Qaderi, "Polyethylene Glycol Diacrylate (PEGDA) Resin Development for 3D-Printed Microfluidic Devices," 2015.